Pergamon

A FORMAL DERIVATION AND NUMERICAL MODELLING OF THE IMPROVED BOUSSINESQ EQUATIONS FOR VARYING DEPTH

S. Beji* and K. Nadaoka†

*Department of Naval Architecture and Ocean Engineering, Istanbul Technical University, Maslak 80626 Istanbul, Turkey.
†Department of Civil Engineering, Tokyo Institute of Technology, 2-12-1 O-okayama, Meguro-ku, Tokyo 152 Japan.

Abstract—A formal derivation of the improved Boussinesq equations of Madsen and Sørensen (1992) is presented to provide the correct forms of the depth-gradient related terms. Linear shoaling characteristics of the new equations are investigated by the method of Madsen and Sørensen (1992) and by the energy flux concept separately and found to agree perfectly, whereas these approaches give conflicting results for the equations derived by Madsen and Sørensen (1992). Furthermore, Nwogu's (1993) modified Boussinesq model is found to produce a linear shoaling-gradient identical with the present work. Numerical modelling of the derived equations for directional waves is carried out by three-time-level finite-difference approximations. A higher-order radiation condition is implemented for effective absorption of the outgoing waves. Several test cases are included to demonstrate the performance of the model. Copyright © 1996 Elsevier Science Ltd

NOMENCLATURE

a: spatially varying wave amplitude,
c: phase velocity vector (c_x, c_y),
g: gravitational acceleration,
h: water depth from still water level,
i: running index for spatial increments in x-direction,
j: running index for spatial increments in y-direction,
k: running index for time increments and magnitude of wave-number vector,
$\mathbf{k}$:   wave-number vector (k_x, k_y),
t: time,
u: depth-averaged horizontal velocity vector (u, v),
u: depth-averaged velocity component in the x-direction,
v: depth-averaged velocity component in the y-direction,
β: dispersion coefficient,
η: surface displacement as measured from still water level,
λ_o: wavelength at the incoming boundary.

1. INTRODUCTION

Due to strong interactions with bottom topography, waves observed in the nearshore zone are almost always nonlinear and, as it is obvious from the frequent occurrence of white-capping and breaking, nonlinearity is usually quite high. Realistic modeling of these waves must therefore account for these nonlinear interactions. At present weakly-nonlinear

weakly-dispersive wave models, namely the Boussinesq-type models, appear to be the most promising ones for practical applications. These depth-integrated equations at once reduce a three-dimensional problem to an equivalent (within the approximations made) two-dimensional problem. Such a reduction in dimension provides significant savings in computation time as well as a certain robustness originating from the simplified numerical procedure. Despite these advantages the Boussinesq equations suffer from the inherent disadvantage of being shallow water equations. To extend their applicable range numerous attempts have been made (Witting, 1984; Madsen et al., 1991; Nwogu, 1993).

Madsen and Sørensen (1992), hereafter referred to as MS, introduced an extension of their improved Boussinesq equations (Madsen et al., 1991) to incorporate varying depth. Their procedure however was found to produce a conflicting result when applied to the Boussinesq equations expressed in terms of the mean velocity (Beji and Battjes, 1994) instead of the depth-integrated velocity as used by MS. More explicitly, when the Boussinesq equations in terms of the mean velocity are improved by MS' technique, the transformed forms (to the depth-integrated velocity) of these equations do not agree with those of MS, who obtained their equations by applying the same technique to the equations formulated in terms of the depth-integrated velocity. Here, a formal derivation is offered to terminate this ambiguity. The resulting momentum equation differs from that of MS with respect to the depth-gradient terms which are the source of the inconsistency mentioned. The correctness of the present derivation is ascertained by showing its perfect agreement with the constancy of energy flux.

The wave equations are discretized via three-time-level finite-difference approximations so that the nonlinear terms could be treated as quasi-linear contributions. The second-order radiation condition of Engquist and Majda (1977) is implemented for a better absorption of the directional waves and found to be quite satisfactory.

2. IMPROVED BOUSSINESQ EQUATIONS FOR SLOWLY VARYING DEPTH

While it is perfectly allowable to *replace* the terms of second-order with their equivalents in the Boussinesq-type equations (see the comments in Peregrine, 1967 and Mei, 1983, p.550 for various forms of the KdV equation) it is questionable to *add* the terms of second-order (on the premise that they are small) to such conservation equations. Replacing the terms of second-order with their equivalents as obtained from the first-order relations has its justification in the derivation process itself, as these equations are the result of an ordering process with respect to two parameters, ε and μ^2, which are assumed to be small. Here ε $(= a/h)$ is defined as the ratio of a typical wave amplitude to the undisturbed depth while μ $(=2\pi h/\lambda)$ is basically the ratio of the undisturbed depth to a typical wavelength. Thus, while the process of adding some second-order terms is in essence of heuristic nature hence liable to inconsistencies; the process of replacing the second-order terms is an approximation permissible within the formal procedure and therefore free of inconsistencies. Here, by performing a simple algebraic manipulation and replacing some second-order terms using a first-order relation we shall derive the improved Boussinesq equations for varying bathymetry. The present work may be viewed as a rectified version of MS' pioneering work, producing a wave model with improved dispersion characteristics such that waves with wavelengths equal to depth may be represented with acceptable errors in amplitude and celerity. For varying depth the linear shoaling is accur-

ate only if depth to wavelength ratio at the incoming boundary is less than 1/4, as demonstrated in section **4**.

We begin by recalling the Boussinesq equations for slowly varying depth (Peregrine, 1967):

$$u_t + (u.\nabla)u + g\nabla\eta = \frac{h}{2} \nabla[\nabla.(hu_t)] - \frac{h^2}{6} \nabla(\nabla.u_t) \tag{1}$$

$$\eta_t + \nabla.[(h + \eta)u] = 0 , \tag{2}$$

where $u =(u,v)$ is the two-dimensional depth-averaged velocity vector, η is the surface displacement, $h = h(x,y)$ is the varying water depth as measured from the still water level, and g is the gravitational acceleration. The subscript t stands for partial differentiation with respect to time and ∇ for the two-dimensional horizontal gradient operator.

By an elementary addition and subtraction process Equation (1) may be re-written as

$$u_t + (u.\nabla)u + g\nabla\eta = (1 + \beta) \frac{h}{2} \nabla[\nabla.(hu_t)] - \beta \frac{h}{2} \nabla[\nabla.(hu_t)] \tag{3}$$
$$- (1 + \beta) \frac{h^2}{6} \nabla(\nabla.u_t) + \beta \frac{h^2}{6} \nabla(\nabla.u_t) ,$$

where β is a scalar to be determined later. Contrary to the usual practice of a full replacement, our aim here is to facilitate a *partial replacement* of the dispersion terms to arrive at a form with better dispersion characteristics. As indicated by Peregrine (1967) the form of the second-order (nonlinear and dispersion) terms may be varied by using the first order relations:

$$u_t + g\nabla\eta = 0, \quad \eta_t + \nabla.(hu) = 0 . \tag{4}$$

We use the first equation in Equation (4), $u_t = -g\nabla\eta$, for replacing the terms proportional to β (we could of course do otherwise and replace the terms proportional to 1+ β) in Equation (3) and obtain

$$u_t + (u.\nabla)u + g\nabla\eta = (1 + \beta) \frac{h}{2} \nabla[\nabla.(hu_t)] + \beta \frac{gh}{2} \nabla[\nabla.(h\nabla\eta)] \tag{5}$$
$$- (1 + \beta) \frac{h^2}{6} \nabla(\nabla.u_t) - \beta \frac{gh^2}{6} \nabla(\nabla^2\eta) ,$$

which is a momentum equation with *mixed* dispersion terms (i.e., the right-hand side contains the derivatives of both u and η). Note that while setting $\beta = 0$ recovers the original equation, $\beta = -1$ corresponds to replacing u_t with $-g\nabla\eta$ in Equation (1) (a full replacement of the dispersion terms).

Equation (2) and Equation (5) then constitute the improved Boussinesq equations for variable depth. When compared with the derivations of similar type equations (Madsen and Sørensen, 1992; Nwogu, 1993) the briefness of the above procedure is remarkable.

The same procedure can be applied to the KdV equation as well; see the appendix for an application.

Equation (5) differs from MS' momentum equation only with respect to the depth-gradient terms produced by the first and second terms on the right. Although the difference may not appear major it is this difference that makes the present model a consistent one. To complete the formulation it is necessary to specify the parameter β in an appropriate way, which is considered next.

3. SPECIFICATION OF DISPERSION PARAMETER

In linearized forms Equation (2) and Equation (5) yield the following dispersion relation

$$\frac{\omega^2}{gk} = \frac{kh(1 + \beta k^2 h^2/3)}{[1 + (1 + \beta)k^2 h^2/3]},$$ (6)

where ω is the cyclic wave frequency, $k^2 = k_x^2 + k_y^2$ and k_x, k_y are the components of the wave-number vector k in the x- and y-directions respectively.

At this stage it should be emphasized that the dispersion relation given by Equation (6) is indeed identical with MS' dispersion relation when B is set to $\beta/3$ in their formulation and Nwogu's dispersion relation when α is set to $-(1+ \beta)/3$ in his formulation. Thus, by specifying these parameters in accord it is possible to make the dispersion relations of these three models identical. This in turn asserts that all these models would have identical group velocities as long as the dispersion parameters are specified concordantly. Basically there are two different ways of specifying the dispersion parameter: matching the resulting dispersion relation with a second-order Padé expansion of the linear theory dispersion relation (Witting, 1984; Madsen and Sørensen, 1992) or minimizing the errors in phase or group speed within a preset range (Madsen *et al.*, 1991; Nwogu, 1993; Chen and Liu, 1995). Since the outcome of one procedure differs only slightly from that of the other the choice does not make a crucial difference. Here, the first approach is preferred and β is determined from the second-order Padé expansion of the linear theory dispersion relation $\omega^2/gk = \tanh kh$:

$$\frac{\omega^2}{gk} = \frac{kh + k^3 h^3/15}{1 + 2k^2 h^2/5},$$ (7)

which requires $\beta = 1/5$ in order that Equation (6) be identical with Equation (7). This specification has the appealing feature of being in accord with the basic underlying derivation procedure of the Boussinesq equations that it is an asymptotic expansion near the long-wave limit (see also the remarks by MS). Fig. 1 compares the dispersion curves for $\beta = 0$, -1, $1/2$, $1/5$ (each one corresponding to a different asymptotic expansion of $\omega^2/gk = \tanh kh$ for small kh) with the exact expression of linear theory. Among these various asymptotic expansions, clearly the one corresponding to the Padé type expansion is the best and should be preferred. Thus, with the specification of β as $1/5$ the new model may propagate relatively shorter waves ($h/\lambda = 1$) with acceptable errors in amplitude and celerity. In this work $\beta = 1/5$ is used throughout, which corresponds to $B = 1/15$ in MS' model and $\alpha = -2/5$ in Nwogu's model.
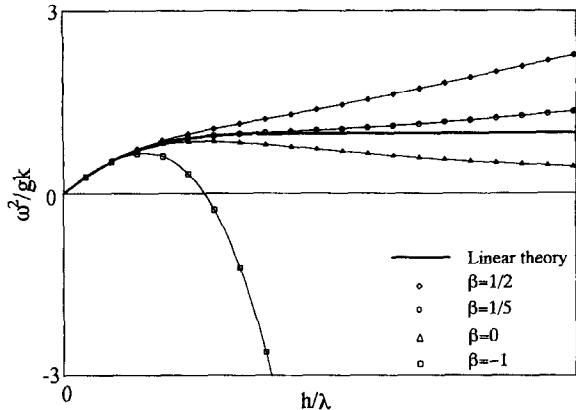
Fig. 1. Dispersion curves for various values of dispersion parameter β compared with linear theory.

4. LINEAR SHOALING CHARACTERISTICS OF IMPROVED BOUSSINESQ EQUATIONS

A linear shoaling analysis of the unidirectional versions of Equation (2) and Equation (5) is now carried out by using two different approaches; that is, the method proposed by MS, and the energy flux concept. The reason of using two different methods is to show that the results do agree for the equations derived here, as they must, but produce conflicting results for the equations derived by MS. The method proposed by MS is employed first; for further details the reader is directed to this particular reference. The linearized forms of the one-dimensional continuity and momentum equations are combined to obtain a single equation for the surface displacement:

$$\eta_{tt} - gh\eta_{xx} + \frac{\beta}{3} gh^3\eta_{xxxx} - \frac{(1 + \beta)}{3} h^2\eta_{xxtt}$$
$$= h_x[g\eta_x + (1 + \beta)h\eta_{xtt} - 2\beta gh^2\eta_{xxx}] , \tag{8}$$

where the subscripts denote partial differentiation with respect to the indicated variable as stated before. A solution of the form $\eta = a(x) \exp [i(\omega t - \varphi(x))]$ is then substituted into Equation (8). Here $a(x)$ represents the amplitude variation due to varying depth and $\varphi(x) = \int k(x)dx$ is the phase function which incorporates the effect of change in wave-number. The zeroth-order terms obtained after substitution give the dispersion relation stated in Equation (6). The first-order terms on the other hand result in a relationship among the amplitude-gradient, wave-number-gradient, and depth gradient. As the final step, the linear dispersion relation is used to express the wave-number-gradient in terms of the depth-gradient so that a relationship between the amplitude-gradient and the depth-gradient may be established:

$$\frac{a_x}{a} = - \frac{(c_3 - c_2c_4)}{c_1} \frac{h_x}{h} \tag{9}$$

in which the coefficients are given by

$$c_1 = 2[1 + 2\beta k^2h^2/3 + \beta(1 + \beta)k^4h^4/9]$$
$$c_2 = [1 + 2\beta k^2h^2 + 5\beta(1 + \beta)k^4h^4/9]$$

$$c_3 = [1 + 2(2\beta - 1)k^2h^2/3 + \beta(1 + \beta)k^4h^4/3]$$

$$c_4 = \frac{1}{2}\left[\frac{1 + (2\beta - 1)k^2h^2/3 + \beta(1 + \beta)k^4h^4/9}{1 + 2\beta k^2h^2/3 + \beta(1 + \beta)k^4h^4/9}\right]. \qquad (10)$$

In Fig. 2 the variation of the shoaling-gradient coefficient $(c_3 - c_2 c_4)/c_1$ as a function of h/λ_0 for different values of the dispersion parameter is plotted against the exact expression of linear theory obtained from the constancy of energy flux using the Stokes' first-order theory for the group velocity C_g. As in Fig. 1, $\beta = 1/5$ is the best choice; however, unlike dispersion characteristics, the linear shoaling is accurate only for $h/\lambda_0 < 1/4$ where λ_0 is the wavelength at the incoming boundary.

A crucial point to note in Equation (10) is that the limiting cases of $\beta = 0$ (the original set of equations) and $\beta = -1$ (full replacement of the dispersion term) result in the elimination of all the fourth-order terms. This must be so because for these degenerate cases the dispersion relation is of an order lower in accuracy.

The constancy of energy flux may also be used in deriving the linear shoaling-gradient for Equation (2) and Equation (5). The result obtained from such a derivation must be identical with Equation (9) and Equation (10), if Equation (2) and Equation (5) are the results of a consistent derivation procedure. Let us then begin by stating the constancy of energy flux in the x-direction

$$\frac{\partial}{\partial x}(a^2 C_g) = 0, \qquad (11)$$

where $a = a(x)$ is the spatially varying wave amplitude as used before and C_g is the group velocity. The shoaling-gradient that the differential equations must possess will be obtained when C_g derived from Equation (6) is used in Equation (11). It is now re-stated that the three models (the present one, MS', and Nwogu's) have identical C_p and C_g for $\beta = 1/5$, $B = 1/15$, and $\alpha = -2/5$ as indicated before.
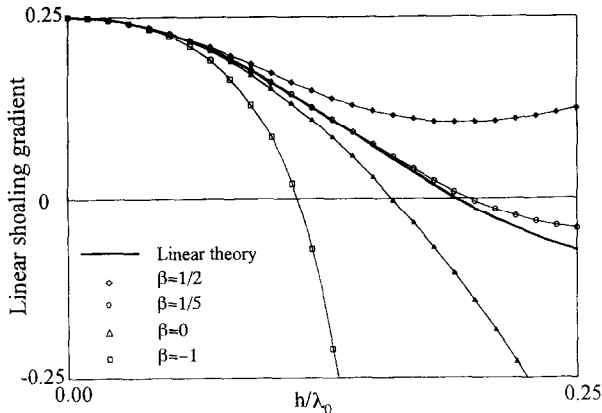
Fig. 2. Variation of the shoaling-gradient coefficient $(c_3 - c_2 c_4)/c_1$ as a function of h/λ_0 for various values of dispersion parameter β compared with the expression according to linear theory.

Equation (11) may be re-expressed as

$$\frac{a_x}{a} = -\frac{1}{2}\frac{(C_g)_x}{C_g}.$$ (12)

We need to compute $(C_g)_x/C_g$ from Equation (6). Differentiating Equation (6) with respect to k and re-arranging give

$$\frac{\omega}{g}C_g = \frac{kh + 2\beta k^3 h^3/3 + \beta(\beta + 1)k^5 h^5/9}{[1 + (\beta + 1)k^2 h^2/3]^2}$$ (13)

Differentiating Equation (13) with respect to x, while noting $d\omega/dx =0$, results in

$$\frac{\omega}{g}(C_g)_x = \frac{(kh)_x[1 + (\beta - 1)k^2 h^2 + \beta(\beta + 1)k^4 h^4/3 + \beta(\beta + 1)^2 k^6 h^6/27]}{[1 + (\beta + 1)k^2 h^2/3]^3}.$$ (14)

Forming the ratio Equation (14)/Equation (13) gives

$$\frac{(C_g)_x}{C_g} = \frac{(kh)_x[1 + (\beta - 1)k^2 h^2 + \beta(\beta + 1)k^4 h^4/3 + \beta(\beta + 1)^2 k^6 h^6/27]}{(kh)[1 + 2\beta k^2 h^2/3 + \beta(\beta + 1)k^4 h^4/9][1 + (\beta + 1)k^2 h^2/3]}.$$ (15)

The final step is to manipulate the ratio $(kh)_x/(kh)$ by expressing k_x/k in terms of h_x/h so that $(kh)_x/(kh)$ may be expressed in terms of h_x/h. To this end first we note $(kh)_x/(kh)$ $= k_x/k + h_x/h$ and then use $d\omega/dx =0$ to obtain

$$\frac{k_x}{k} = -\frac{1}{2}\frac{[1 + (2\beta - 1)k^2 h^2/3 + \beta(\beta + 1)k^4 h^4/9]}{[1 + 2\beta k^2 h^2/3 + \beta(\beta + 1)k^4 h^4/9]}\frac{h_x}{h}.$$ (16)

Using Equation (16) in Equation (15) and then substituting Equation (15) into Equation (12) one gets the amplitude-gradient in terms of the depth-gradient

$$\frac{a_x}{a} = -\frac{(1 + \beta k^2 h^2/3)[1 + (\beta-1)k^2 h^2 + \beta(\beta + 1)k^4 h^4/3 + \beta(\beta + 1)^2 k^6 h^6/27]}{4[1 + 2\beta k^2 h^2/3 + \beta(\beta + 1)k^4 h^4/9]^2}\frac{h_x}{h},$$ (17)

which is the true expression obtained from the constancy of energy flux.
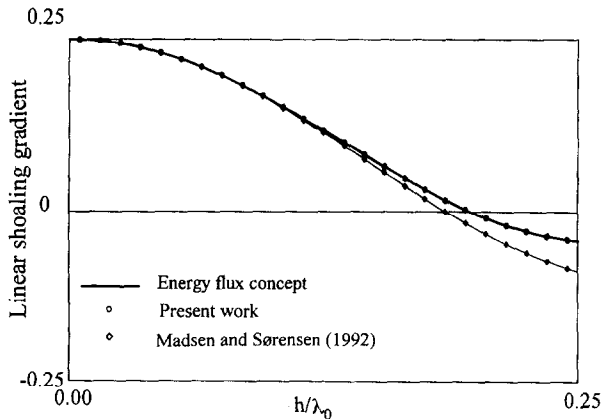
Fig. 3. Variation of the shoaling-gradient coefficient of the present work and of Madsen and Sørensen (1992) compared with the expression obtained from the energy flux concept.

In Fig. 3 the shoaling-gradient coefficient of Equation (17) (for $\beta = 1/5$) is compared with that of Equation (9) and with the corresponding expression of MS. As it is seen, Equation (17) produces identical results (solid line) with Equation (9) (circles) while MS' formulation (triangles) diverges. The exact analytical correspondence of Equation (17) with Equation (9) may also be established; however the algebra is complicated and therefore it is not repeated here. Likewise, it can analytically be shown that the expression given by MS is at variance with Equation (17). On the other hand, the linear-shoaling gradient coefficient of Nwogu's equations is found to be identical with the present one. Compared with Nwogu's equations the advantage of Equation (2) and Equation (5) is basically due to the conservation form of Equation (2) which is most suitable for accurate computations.

5. NUMERICAL MODELLING

5.1. *Discretization of governing equations*

In discretizing time-dependent nonlinear partial differential equations via finite-difference approximations a straightforward way of handling the nonlinear terms is to adopt a three-time-level formulation. Following this line, such an approach is employed here; both space and time derivatives are centered and η, u, v are all placed at the same grid points, according to the pure leap-frog method.

To reduce the computational effort the solution process is decoupled so that only one variable is solved along each row or column until the entire domain is covered. The x-momentum equation is solved for u, the y-momentum equation for v. Such artificial decoupling of course necessitates some approximations and these are indicated below. Continuity equation does not require any additional approximation as it is possible to implement an explicit discretization. For brevity, only time derivatives are given in discretized forms. All spatial derivatives are approximated by centered difference formulations. The x-sweep equation is

$$
\begin{aligned}
&\frac{(u^{k+1} - u^{k-1})}{2\Delta t} - (1 + \beta) \left[\frac{h^2}{3} \frac{(u_{xx}^{k+1} - u_{xx}^{k-1})}{2\Delta t} + hh_x \frac{(u_x^{k+1} - u_x^{k-1})}{2\Delta t} \right] \\
&= -g\eta_x^k - \frac{1}{2}(u^2 + v^2)_x^k + (1 + \beta)\frac{h^2}{3} \frac{(v_{xy}^{k+1} - v_{xy}^{k-1})}{2\Delta t} \\
&+ \frac{1}{2}(1 + \beta) \left[hh_x \frac{(v_y^{k+1} - v_y^{k-1})}{2\Delta t} + hh_y \frac{(v_x^{k+1} - v_x^{k-1})}{2\Delta t} \right] \\
&+ \beta g \frac{h^2}{3}(\eta_{xxx}^k + \eta_{xyy}^k) + \beta gh(h_x\eta_{xx}^k + \frac{1}{2}h_y\eta_{xy}^k + \frac{1}{2}h_x\eta_{yy}^k) ,
\end{aligned}
\tag{18}
$$

in which the superscript k denotes the time level. Note that to improve the computational accuracy the nonlinear terms are re-expressed by using the irrotationality condition $u_y = v_x$.[1] Also, the three-point-averaging formulation of Zabusky and Kruskal (1965) is used in the evaluation of the spatial derivatives of these terms, as it improves the robustness of the scheme. The new time level values v^{k+1}'s appearing on the right-hand side of Equation (18) are treated as known by using the last computed values so that u^{k+1}'s are the

---

[1] Strictly speaking this is not valid for a varying depth but an acceptable approximation. See Peregrine (1967).

only unknowns. The resulting matrix equation is tridiagonal and can be solved very efficiently by the Thomas algorithm.

Similarly the y-sweep is

$$
\frac{(v^{k+1} - v^{k-1})}{2\Delta t} - (1 + \beta) \left[\frac{h^2 (v_{yy}^{k+1} - v_{yy}^{k-1})}{3} + hh_y \frac{(v_y^{k+1} - v_y^{k-1})}{2\Delta t} \right]
$$

$$
= - g\eta_y^k - \frac{1}{2} (u^2 + v^2)_y^k + (1 + \beta) \frac{h^2}{3} \frac{(u_{xy}^{k+1} - u_{xy}^{k-1})}{2\Delta t} \tag{19}
$$

$$
+ \frac{1}{2} (1 + \beta) \left[hh_y \frac{(u_x^{k+1} - u_x^{k-1})}{2\Delta t} + hh_x \frac{(u_y^{k+1} - u_y^{k-1})}{2\Delta t} \right] + \beta g \frac{h^2}{3} (\eta_{yyy}^k
$$

$$
+ \eta_{xxy}^k) + \beta g h (h_y \eta_{yy}^k + \frac{1}{2} h_x \eta_{xy}^k + \frac{1}{2} h_y \eta_{xx}^k) ,
$$

in which v^{k+1}s are the only unknowns. The u^{k+1}s and subsequently v^{k+1}s obtained from respectively Equation (18) and Equation (19) are only first estimates since these variables are computed separately. It is therefore necessary to iterate to obtain accurate results. For the computational tests presented later a single iteration was found to be sufficient (no improvements were observed with further iterations) but more complicated problems may require two iterations.

The surface displacement is obtained from an explicit discretization of the continuity equation:

$$
\frac{(\eta^{k+1} - \eta^{k-1})}{2\Delta t} + [(h + \eta)u]_x^k + [(h + \eta)v]_y^k = 0 . \tag{20}
$$

5.2. *Boundary conditions*

Boundary conditions at the rigid impermeable bottom and the free surface are automatically satisfied by the governing equations. It then remains to specify the conditions at the boundaries vertically enclosing the physical domain of interest. A boundary along which the incident wave field is introduced is quite easy to deal with. An absorbing boundary on the other hand is the source of a major difficulty in any numerical wave model and therefore requires particular attention.

Engquist and Majda (1977) introduced a systematic approach which can produce successively higher-order absorbing boundary conditions. For a non-dispersive wave equation $w_{tt} - w_{xx} - w_{yy} = 0$ (here w represents either velocity or surface displacement) their first-order approach leads to the well-known Sommerfeld radiation condition which is appropriate for normally impinging waves. The second-order approximation on the other hand produces the following formula for waves traveling in the positive x-direction.

$$
w_{tt} + w_{xt} - \frac{1}{2} w_{yy} = 0 . \tag{21}
$$

At the lowest order, when combined with Equation (2), Equation (5) is equivalent to the non-dispersive wave equation with a wave propagation celerity $c = \sqrt{gh}$. It is then a plausible approximation to use the dimensional form of Equation (21) with the celerity c

= √gh as the radiation condition in solving Equation (5). Thus, for waves propagating in the positive x-direction with the phase celerity c we employ the following radiation condition for the x-component of the velocity $u(u,v)$:

$$u_{tt} + cu_{xt} - \frac{1}{2} c^2 u_{yy} = 0 .$$ (22)

If the waves are moving in the negative x-direction the sign in front of the second term reverses. The expressions corresponding to the v-component of the velocity are analogous.

The radiation condition stated in Equation (22) is discretized by centered-differences in time and in the y-direction while backward-difference formulation is used in the x-direction:

$$\frac{(u_{i,j}^{k+1} - 2u_{i,j}^{k} + u_{i,j}^{k-1})}{\Delta t^2} + c \frac{(u_{i,j}^{k+1} - u_{i-1,j}^{k+1}) - (u_{i,j}^{k-1} - u_{i-1,j}^{k-1})}{2\Delta x \Delta t}$$
$$- \frac{1}{2} c^2 \frac{(u_{i,j+1}^{k} - 2u_{i,j}^{k} + u_{i,j-1}^{k})}{\Delta y^2} = 0 \text{ for } i = n ,$$ (23)

where i and j label the spatial points in the $x - y$ Cartesian system and i=n corresponds to a node on the boundary. Note that Equation (23) is valid for waves propagating in the positive x-direction. Details about the boundary conditions can be found in Beji and Nadaoka (1994).

5.3. Initial condition

All computations are started by specifying u, v and η over the entire domain for the first two time levels. Except for the ring test which is presented later as an example, the initial condition is the state of rest; that is, both the velocity field and the surface displacement are zero throughout the domain.

6. NUMERICAL SIMULATIONS

The performance of the numerical scheme described above is now illustrated for two selected cases. The first case is the ring test which provides a check for the symmetrical accuracy of the numerical model as well as allowing comparisons for the first- and second-order radiation conditions. A surface elevation of solitary-wave shape is initially imposed and then the computation is let to proceed on its due course. The initial wave height to depth ratio is 0.3. The computational area is 2m ×2m, which is discretized by 50 points along both x- and y-axes. The time step is 1/25 second. The left column in Fig. 4 shows the computational results with the first-order boundary condition at t =1/2, 1, and 2 seconds respectively. On the right column the corresponding results with the second-order boundary condition are depicted. As it is obvious from the surface profiles at t =2 seconds the first-order boundary condition is inferior, especially at the corners of the computational domain where the radiating wave direction makes the sharpest angle with the boundaries.

The second case is the computation of wave convergence over a bottom topography that acts as a focusing lens (Whalin, 1971). The wave tank used in the experiments was 25.6m long and 6.096m wide. In the middle portion of the tank eleven semicircular steps were evenly spaced to form a topographical lens. The equations describing the topography are given as follows (Whalin, 1971):
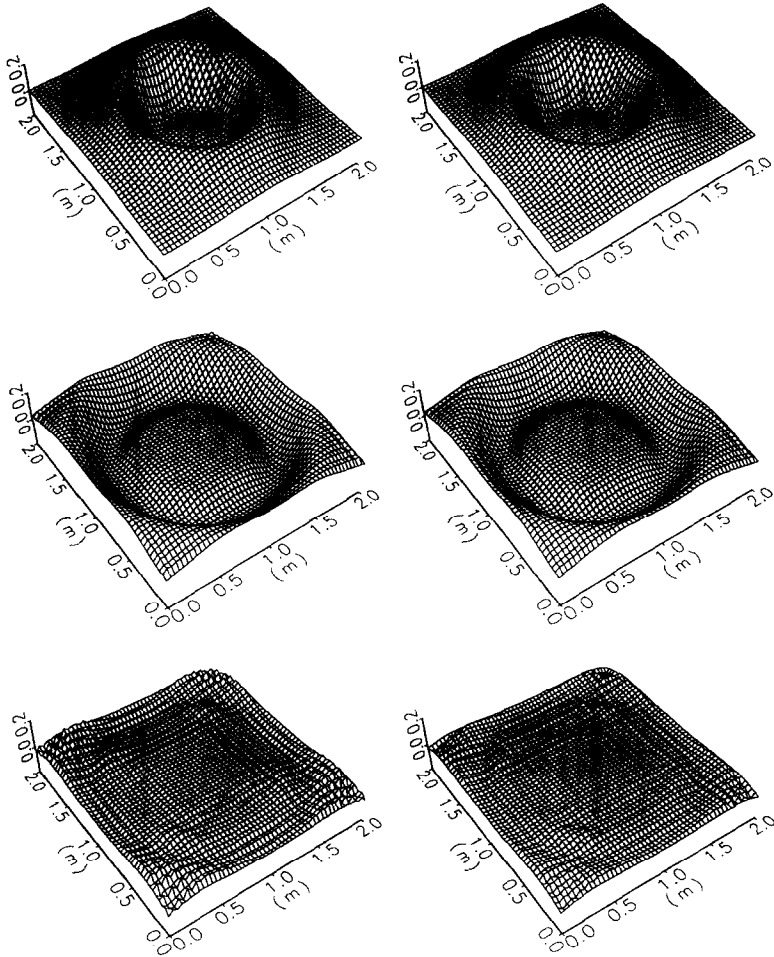
Fig. 4. Ring test displayed at $t = 1/2$, 1, 2 seconds. Left column: the first-order radiation condition, right column: the second-order radiation condition.

$$h(x,y) = \begin{cases} 0.4572 & \text{for } 0 \leqslant x < 10.67 - G \\ 0.4572 + (10.67 - G - x)/25 & \text{for } 10.67 - G \leqslant x < 18.29 - G \\ 0.1524 & \text{for } 18.29 - G \leqslant x \leqslant 21.34 \end{cases} \qquad (24)$$

where

$$G(y) = [y(6.096 - y)]^{1/2} \quad \text{for } 0 \leqslant y \leqslant 6.096 , \qquad (25)$$

in which all the variables are in meters. Three sets of experiments were conducted by generating waves with periods $T = 1$, 2, and 3 seconds and the harmonic amplitudes along the centerline of the wave tank were measured at various stations.

For all three cases the computations were performed with a span-wise resolution Δy of 1/14 of the wave tank width. Since the bathymetry is symmetric with respect to the center-

line, only one-half of the tank is discretized. The no-flux boundary conditions are used along the centerline and the side-wall. Figure 5a compares the computed harmonic amplitudes with the measured data for the incident wave period $T = 1$ second and the wave amplitude $a_0 = 1.95$ cm. The time-step and the x-direction resolution were $\Delta t = T/35$ and
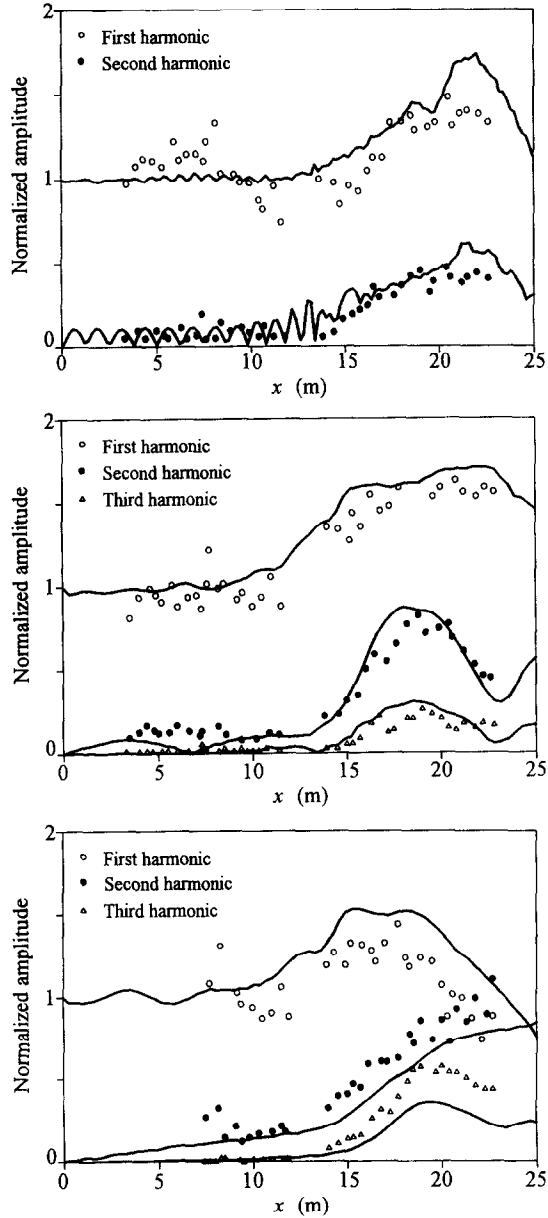
Fig. 5. a. Whalin's (1971) test for incident waves of $T = 1$ second. Measured and computed wave amplitudes along the centerline of the wave tank. Solid line: computation, scatter: experimental data; b. Same as in Figure 5a but for incident waves of $T = 2$ seconds; c. Same as in Figure 5b but for incident waves of $T = 3$ seconds.
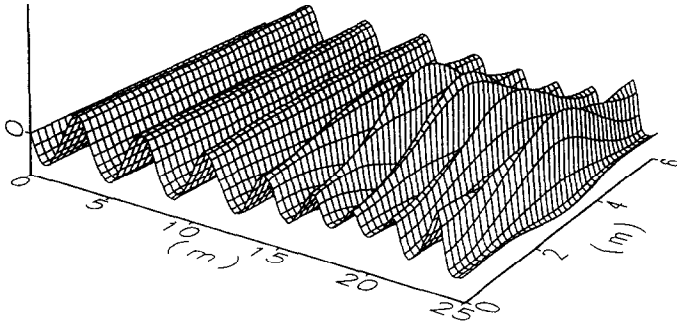
Fig. 6. A perspective view of the fully-developed wave field for incident waves of T =2 seconds. Corresponds to Figure 5b.

$\Delta x = \lambda_m/25$ with λ_m denoting the mean wavelength computed as the average of the deep-water and shallow-water wavelengths. In Fig. 5b the case for T =2 seconds and a_0=0.75 cm shown, the resolutions were $\Delta t = T/35$ and $\Delta x = \lambda_m/35$. Fig. 5c gives the comparisons for T =3 second waves with the deep water amplitude a_0=0.68 cm. Since the harmonic amplitudes were comparable with the primary wave amplitude, it was necessary to adopt somewhat higher resolutions and therefore $\Delta t = T/45$ and $\Delta x = \lambda_m/45$ for this last case. Finally, in Fig. 6 a perspective view of the fully-developed wave field is depicted for T =2 second waves to give an idea about the wave patterns. Despite some discrepancies the overall model predictions agree with the measurements hence give confidence for the wave model.

7. CONCLUDING REMARKS

A formal derivation of the improved Boussinesq equations has been presented to terminate the consistency problems arising from the heuristic derivation procedure of MS. The present study should be viewed as a rectification of their pioneering work and an attempt to establish firmer grounds for the procedure of extending the applicable range of the Boussinesq equations expressed in terms of a conventional variable such as depth-averaged velocity. It is shown that the derived equations satisfy the energy considerations as well as being in accord with Nwogu's modified Boussinesq equations.

The numerical scheme introduced appears to be good both in terms of accuracy and computational time. Use of the three-time-level formulation not only makes it possible to treat the nonlinear terms in the most straightforward manner but also shortens the computational time considerably by permitting an explicit formulation of the continuity equation as completely decoupled from the momentum equations. The absorption of the outgoing waves that approach in a multitude of directions is a delicate problem. The higher-order radiation condition used here is found to be reliable in simulations even with acute angles of wave radiation as demonstrated by the ring test.

REFERENCES

Beji, S. and Battjes, J.A. 1994. Numerical simulation of nonlinear wave propagation over a bar. *Coastal Eng.* **23**, 1–16.

Beji, S. and Nadaoka, K. 1994. Numerical simulation of nonlinear directional waves by an improved Boussinesq model. *Proc. Int. Symp. Waves–Physical and Numerical Modeling, Vancouver, Canada* **1**, 534–543.

Chen, Y. and Liu, P.L.-F. 1995. Modified Boussinesq equations and associated parabolic models for water wave propagation. *J. Fluid Mech.* **288**, 351–381.

Engquist, B. and Majda, A. 1977. Absorbing boundary conditions for the numerical simulation of waves. *Math. Comp.* **31**, 629–651.

Madsen, P.A., Murray, R. and Sørensen, O.R. 1991. A new form of the Boussinesq equations with improved linear dispersion characteristics. *Coastal Eng.* **15**, 371–388.

Madsen, P.A. and Sørensen, O.R. 1992. A new form of the Boussinesq equations with improved linear dispersion characteristics. Part 2: A slowly-varying bathymetry. *Coastal Eng.* **18**, 183–204.

Mei, C.C. 1983. *The Applied Dynamics of Ocean Surface Waves* (740 pp.). John Wiley and Sons.

Nwogu, O. 1993. Alternative form of Boussinesq equations for nearshore wave propagation. *J. Waterway, Port, Coastal, and Ocean Eng.* **119**, 618–638.

Peregrine, D.H. 1967. Long waves on a beach. *J. Fluid Mech.* **27**, 815–827.

Whalin, R. W. 1971. *The Limit of Applicability of Linear Wave Refraction Theory in a Convergence Zone.* Res. Rep. H-71-3, U.S. Army Corps of Engrs, Waterways Expt. Station, Vicksburg, M.S.

Witting, J.M. 1984. A unified model for the evolution of nonlinear water waves. *J. Comp. Phys.* **56**, 203–236.

Zabusky, N.J. and Kruskal, M.D. 1965. Interaction of solitons in a collisionless plasma and recurrence of initial states. *Phy, Rev. Lett.* **15**, 240.

APPENDIX

Consider the KdV equation:

$$\eta_t + c_0\eta_x + \frac{3c_0}{2h}\eta\eta_x - \frac{h^2}{6}\eta_{xxt} = 0 \,, \tag{A1}$$

where $c_0=(gh)^{1/2}$ is the non-dispersive wave celerity. Equation (A1) may be rewritten as

$$\eta_t + c_0\eta_x + \frac{3c_0}{2h}\eta\eta_x - (1 + \beta)\frac{h^2}{6}\eta_{xxt} + \beta\frac{h^2}{6}\eta_{xxt} = 0 \,, \tag{A2}$$

in which β is for the time being an undetermined parameter. We use the linearized non-dispersive form of the KdV, $\eta_t + c_0\eta_x = 0$, to replace the last term in Equation (A2) $\eta_{xxt} = -c_0\eta_{xxx}$ and obtain

$$\eta_t + c_0\eta_x + \frac{3c_0}{2h}\eta\eta_x - (1 + \beta)\frac{h^2}{6}\eta_{xxt} - \beta c_0\frac{h^2}{6}\eta_{xxx} = 0 \,. \tag{A3}$$

The linear dispersion relation corresponding to Equation (A3) is

$$\frac{\omega}{\sqrt{gk}} = \frac{\sqrt{kh}(1 + \beta k^2h^2/6)}{[1 + (1 + \beta)k^2h^2/6]} \,. \tag{A4}$$

The second-order Padé expansion of $\omega/(gk)^{1/2}=(\tanh kh)^{1/2}$ reads

$$\frac{\omega}{\sqrt{gk}} = \sqrt{\tanh kh} \simeq \frac{\sqrt{kh(1 + k^2h^2/15)}}{\sqrt{1 + 2k^2h^2/5}} \simeq \frac{\sqrt{kh}(1 + k^2h^2/30)}{1 + k^2h^2/5} \tag{A5}$$

where use has been made of the approximation $(1+\xi)^{1/2} \simeq 1+\xi/2$ (for small ξ) in evaluating the square roots. In order that Equation (A4) be identical with Equation (A5), β must be 1/5. With this specification, the new KdV equation Equation (A3) has better dispersion characteristics.